Time-Resolved Linewidth Enhancement Factors in Quantum Dot and Higher-Dimensional Semiconductor Amplifiers Operating at 1.55 μm

Aaron J. Zilkie, *Member, IEEE, Member, OSA*, Joachim Meier, Mo Mojahedi, *Senior Member, IEEE*, Amr S. Helmy, *Senior Member, IEEE, Member, OSA*, Philip J. Poole, Pedro Barrios, Daniel Poitras, Thomas J. Rotter, *Member, IEEE, Member, OSA*, Chi Yang, Andreas Stintz, Kevin J. Malloy, *Senior Member, IEEE*, Peter W. E. Smith, *Life Fellow, IEEE, Fellow, OSA*, and J. Stewart Aitchison, *Senior Member, IEEE, Fellow, OSA*

Invited Paper

***Abstract*—We report time-resolved measurements of the linewidth enhancement factors (α-factors) α_{cr}, α_{CH}, and α_{TPA}, associated with the adiabatic carrier recovery, carrier heating, and two-photon absorption dynamical processes, respectively, in semiconductor optical amplifiers (SOAs) with different degrees of dimensionality–one InAs/InGaAsP/InP quantum dot (0-D), one InAs/InAlGaAs/InP quantum dash (1-D), and a matching InGaAsP/InGaAsP/InP quantum well (2-D)—all operating near 1.55-μm wavelengths. We find the lowest α_{cr} values in the QD SOA, 2–10, compared to 8–16 in the QW, and values of α_{CH} and α_{TPA} that are also lower than in the QW. In the QD SOA, the α-factors exhibit little wavelength dependence over the gain bandwidth, promising for wide-bandwidth all-optical applications. We also find significant differences in the α-factors of lasers with the same structure, due to the differences between gain changes that are induced optically or through the electrical bias. For the lasers we find the QW structure instead has the lower α-factor, having implications for directly modulated laser applications.**

***Index Terms*—Linewidth enhancement factor, phase modulation, quantum dots, quantum wells, quantum wires, semiconductor lasers, semiconductor optical amplifiers.**

I. Introduction

THE linewidth enhancement factor, or α-factor, is an important parameter describing the performance of semiconductor lasers and amplifiers in high speed applications. For example, it is a measure of linewidth broadening and chirp in directly modulated lasers [1]–[3], and of the strength of phase effects in semiconductor optical amplifiers (SOAs) in optical signal processing schemes [4]. Low-α-factor directly modulated lasers would enable implementation of high-bit-rate transmitters with a simple architecture in fiber-optic communications networks. Additionally, SOAs with a low α-factor are desired for minimizing chirp and phase nonlinearities during amplification of short pulses. However, in an SOA a large α-factor may also be desired, for example to maximize the modulation efficiency in a cross-phase-modulation based all-optical signal processing device.

Recently, quantum dot (QD) amplifiers have attracted much attention for high-speed applications. This is because the symmetrical nature of their theoretically delta-function-like density of states provides the potential for low or near-zero α-factors [5]. In addition they can have faster gain recovery times and reduced ultrafast transients [6]. QD amplifiers working in the 1.55-μm wavelength window are of particular interest as they could make possible low-α-factor directly modulated laser sources which could be used for optical transmitters in high-speed telecommunications networks.

There have been a number of reports of α-factor measurements in QD lasers operating in the 1.0–1.3-μm wavelength range, a summary of which can be found in [5]. The lowest α-factor recently reported was a value near zero in a tunnel injection QD laser in [7], but generally the values reported have been in the range of 1–3. Values increased up to 10 or greater for high bias currents in some cases however, and additionally they were found to vary with photon energy over the gain bandwidth, and to depend significantly on the energy level structure of the QDs. A few studies comparing the α-factor between QD and quantum well (QW) lasers also found QD laser α-factors to be both lower [8], [9] and higher [10] than those in QW lasers.

The variations in the reported α-factors are partially a result of the influences of the multiple nonlinear processes involved in the gain-index coupling. It is well known, for example, that in a laser the effect of spectral hole burning (SHB) in addition to adiabatic changes in carrier density population result in both "adiabatic" and "transient" chirp terms [11]. However, carrier heating (CH) and two-photon absorption (TPA) are nonlinear processes which additionally have a significant effect on the gain-index response. Thus, a more complete understanding of the α-factor

Manuscript received September 30, 2007; revised February 24, 2008. This work was supported by the National Science and Engineering Research Council, in part through the research network "Agile All-Photonics Networks."

A. J. Zilkie, M. Mojahedi, A. S. Helmy, P. W. E. Smith, and J. S. Aitchison are with the Department of Electrical and Computer Engineering, University of Toronto, Toronto, ON M5S3G4 Canada (e-mail: aaron.zilkie@utoronto.ca).

J. Meier was with the University of Toronto, Toronto, ON M5S3G4 Canada. He is now with High Q Laser Production GmbH, A-6845 Hohenems, Austria.

P. J. Poole, P. Barrios, and D. Poitras, are with the Institute for Microstructural Sciences, National Research Council Canada, Ottawa, ON K1A 0R6 Canada.

T. J. Rotter, C. Yang, A. Stintz, and K. J. Malloy are with the Center for High Technology Materials, University of New Mexico, Albuquerque, NM 87106 USA.

Color versions of one or more of the figures in this paper are available online at http://ieeexplore.ieee.org.

Digital Object Identifier 10.1109/JLT.2008.923215

in a device can be attained if the α-factor can be broken down into values for each of these nonlinear processes [11].

Such a break-up of the α-factors enables one to extract the α-factor components from ultrafast gain and phase measurements in an SOA. This is because in an SOA the material responses can be directly probed in the absence of cavity feedback effects. Despite the many reports referenced above that quote effective α-factors in QD lasers, there have been only a few measurements of the α-factor in QD SOAs [12]–[15], and to our knowledge only one report of a measurement of time-resolved α-factors, in a bulk SOA [4]. Furthermore, there have been no reports, to our knowledge, on the α-factor in InP-based QD lasers and amplifiers operating in the important telecommunications wavelength range. In this paper we present such a report, by giving an analysis of the time-resolved α-factors obtained from 150-fs-resolution heterodyne pump probe measurements in our InP-based QD SOA operating near 1.55-μm wavelengths, as well as in a QDash and matching QW SOA [6]. Additionally, we compare the SOA α-factors to laser α-factors measured in QD and QW lasers with the same structure.

II. The Time-Resolved α-Factors

The α-factor is defined in a semiconductor gain medium as the change in the real part of the susceptibility $\chi_{\rm r}$ per change in carrier density N divided by the associated change in the imaginary part of the susceptibility $\chi_{\rm im}$ per change in carrier density N. This is also equivalent to $4\pi/\lambda$ times the change in the effective refractive index of the optical mode n divided by the associated change in the net modal gain coefficient g:

$$\alpha = \frac{\dfrac{d\chi_r}{dN}}{\dfrac{d\chi_{im}}{dN}} = -\frac{4\pi}{\lambda}\frac{\dfrac{dn}{dN}}{\dfrac{dg}{dN}} = -\frac{4\pi}{\lambda}\frac{\Delta n}{\Delta g} = \frac{-2}{L}\frac{\Delta\phi}{\Delta g}. \quad (1)$$

Here, λ is the vacuum wavelength of the light, L is the device length, and the phase change $\Delta\phi$ is associated with the index change Δn according to $\Delta n = \lambda\Delta\phi/(2\pi L)$. To obtain time-resolved α-factors, the index changes Δn and resulting chirp $\Delta\nu$ in a laser or amplifier can be more generally described by a sum of changes due to each nonlinear effect [4], [11]

$$\begin{aligned}\Delta\nu &= -\frac{v_g}{\lambda}\Delta n \\ &= \frac{v_g}{4\pi}[\alpha_{cr}\Delta g_{cr} + \alpha_{\rm CH}\Delta g_{\rm CH} \\ &\qquad + \alpha_{\rm SHB}\Delta g_{\rm SHB} + \alpha_{\rm TPA}\Delta g_{\rm TPA}]. \end{aligned} \quad (2)$$

In (2), v_g is the photon group velocity, and each α-factor term is determined from the gain changes Δg and index changes Δn due to its corresponding nonlinear process, using (1)

$$\begin{aligned}\alpha_{cr} &= -\frac{4\pi}{\lambda}\frac{\Delta n_{cr}}{\Delta g_{cr}}, \quad \alpha_{\rm CH} = -\frac{4\pi}{\lambda}\frac{\Delta n_{\rm CH}}{\Delta g_{\rm CH}}, \\ \alpha_{\rm SHB} &= -\frac{4\pi}{\lambda}\frac{\Delta n_{\rm SHB}}{\Delta g_{\rm SHB}}, \quad \alpha_{\rm TPA} = -\frac{4\pi}{\lambda}\frac{\Delta n_{\rm TPA}}{\Delta g_{\rm TPA}}. \end{aligned} \quad (3)$$

The Δg and Δn terms with subscript "cr" are the gain and index changes due to only adiabatic changes in carrier density alone, and the terms with subscript "CH", "SHB", and "TPA" are the changes due to each of the carrier heating, spectral hole burning, and two-photon absorption processes alone, respectively. Note that the quantities α_{cr} and $\alpha_{\rm CH}$ are the same as α_N and α_T in [4] and [11].

We employ degenerate heterodyne pump-probe measurements of the gain and refractive index to obtain the time-resolved components of the gain and index changes in (3). Conventional measurements involving DC or RF modulation of the electrical bias are limited to obtaining transient and adiabatic "effective" α-factors on time scales dictated by the system electrical bandwidth and the large-signal modulation speeds. Pump-probe measurements, on the other hand, facilitate extraction of the temporal behavior of the α-factor over subpicosecond timeframes, and under the condition of *optical* excitation, of prime importance for high bit-rate ($\geq$100 Gb/s) all-optical signal processing. These time-resolved α-factors can then be used as parameters for models of SOA dynamics, like those in [11], [16], and [17], for all-optical signal processing applications at 1.55-μm wavelengths. In particular, our heterodyne setup, with its 150-fs resolution and degenerate-wavelength pump and probe, allows us to resolve the CH, SHB, and TPA processes which evolve over a $\sim$1 ps time frame, at the exact wavelength of the pump excitation. Our measurements here represent an improvement over the 3-ps-resolution nondegenerate-wavelength measurements of the time-resolved α-factors reported previously in [4].

III. Samples and Experiment

The details of the sample structures, and of the heterodyne pump-probe setup used to perform the dynamics measurements, can be found in [6]. The QD SOA is a p-i-n ridge-waveguide diode consisting of five stacked layers of self-assembled InAs dots, grown in InGaAsP barrier layers on an exactly oriented (100) InP substrate by chemical beam epitaxy (CBE). It has a ridge width of 2 μm, a length of 1 mm, and its facets are anti-reflection (AR) coated. The QW SOA structure is as similar to the QD SOA as possible to allow for our comparative study, having identical cladding layers and doping, but containing five InGaAsP compressively strained quantum wells in place of the InAs dot layers. The QDash (dash-in-a-well) structure consists of five layers of InAs quantum dashes embedded in AlGaInAs quantum wells separated by AlGaInAs barriers, all grown on an InP substrate. The sample has a 5 μm ridge width, and is 1 mm in length. All three devices have their peak gain near 1550 nm, as can be seen from their amplified spontaneous emission (ASE) spectra (Fig. 1). We have also estimated that the QD structure has its ground state (GS), first excited state (ES1), second excited state (ES2), and third excited state (ES3) at 1665 nm, 1620 nm, 1580 nm, and 1535 nm, respectively [6] (Fig. 5 inset), and that the sum of the inhomogeneous and homogeneous broadening at 300 K for each level is $\sim$24 meV ($\sim$49 nm).

The laser source in the pump-probe experiments is a Ti:sapphire-pumped optical parametric oscillator (OPO) generating nearly Fourier-limited 150 fs pulses at a repetition rate of 76 MHz (spectrum also shown in Fig. 1). The degenerate heterodyne pump-probe experiments provide simultaneous measurement of the amplitude and phase dynamics with 150 fs resolution in the SOAs. For the measurements in all three samples, the pump and probe beams were TE-polarized, and in each case the pump pulse energies entering the waveguides

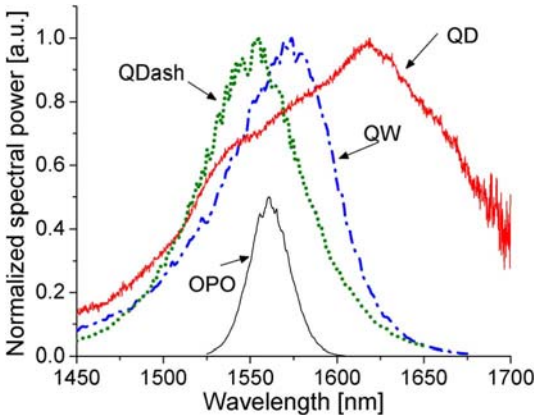

Fig. 1. Normalized ASE spectra of the three SOA samples at maximum bias (QD = thick solid line, QDash = dotted line, QW = dash-dotted line) and the spectrum of the 150 fs OPO pulses (thin solid line), scaled by a factor of 0.5 for clarity.

were set to ∼1 pJ [6], which is ∼1/5 of the 3-dB saturation pulse energies (approximately equal in all three samples), so as to induce similar saturation effects in all three samples and ensure the pump energies were in the small signal regime [16], [18]. The probe pulse energies were also a factor of 10 lower than the pump energies in all the measurements.

IV. SOA α-Factor Analysis

The amplitude and phase dynamics measured in the samples via the heterodyne pump-probe experiments are reported in detail in [6]. Good fits to the amplitude data are obtained by assuming an amplitude impulse response, $h_{\rm amp}$, for the SOAs which consists of exponential terms for the long-lived carrier recovery, carrier heating, and spectral hole burning processes, which have amplitudes a_{cr}, $a_{\rm SHB}$, and $a_{\rm CH}$, respectively, as well as a term for the instantaneous two photon absorption and coherent effects, which has amplitude $a_{\rm inst}$ [19], [20]:

$$h_{\rm amp}=u(t)\left\{a_{cr}\exp(-t/\tau_{cr})+a_{\rm CH}\exp(-t/\tau_{\rm CH})\cdot[1-\exp(-t/\tau_{\rm eff})]+a_{\rm SHB}\exp(-t/\tau_{\rm SHB})+a_{\rm inst}\delta(t)\right\}+1. \quad (4)$$

Here, the carrier heating term is expressed in the "delayed carrier heating" form of [19] and [20], with $1/\tau_{\rm eff}=1/\tau_{\rm SHB}-1/\tau_{\rm CH}$. The time constants were measured to have the values $\tau_{\rm CH}\approx 0.75-2$ ps, $\tau_{\rm SHB}=0.1-0.5$ ps, and $\tau_{cr}=\tau_{ar}=80-500$ ps in the absorption regime, and $\tau_{cr}=\tau_{gr}=560-1500$ ps in the gain regime (see [6]).

Good fits to the phase data were obtained by assuming a similar phase impulse response, $h_{\rm ph}$. Because spectral hole burning has a negligible contribution to the phase changes, since the burning is symmetric about the pump center frequency, the phase impulse response is assumed to be

$$h_{\rm ph}=u(t)\left\{a_{crp}\exp(-t/\tau_{cr})+a_{{\rm CH}p}\exp(-t/\tau_{\rm CH})+a_{{\rm inst}p}\delta(t)\right\}. \quad (5)$$

The amplitude and phase changes due to the perturbation of the pump pulses are then obtained by convolving the impulse responses (4) and (5) with the pump pulse photon density, $S_{\rm pump}(t)$, under the assumption that the gain and phase change linearly with the pump photon density (i.e., assuming small-signal perturbative changes) [18]. This assumption is justified for our relatively weak 1-pJ pulse energies that are ∼1/5 of the saturation pulse energies.

The pump-probe experiments however give the gain changes $\Delta G_{\rm dB}(\tau)=10\log(T/T_0)$ and phase change $\Delta\phi(\tau)$ of the *probe* pulses as a function of pump-probe delay τ however, therefore, this result must be further convolved by the normalized probe photon density $S_{\rm probe}(t)$. Furthermore, the probe pulses are a scaled replica of the pump pulses, therefore $\Delta G_{\rm dB}$ and $\Delta\phi$ can be equivalently obtained by convolving (4) and (5) with the normalized autocorrelation of the laser pulses, $R_S(\tau)$, as long as (4) and (5) are scaled by the integral of the pump pulse photon density S_0

$$\Delta G_{\rm dB}(\tau)=10\log\left[\frac{T(\tau)}{T_0}\right]=10\log(e)\Delta gL=h_{\rm amp}(\tau)S_0*R_S(\tau) \quad (6)$$

$$\Delta\phi(\tau)=h_{\rm ph}(\tau)S_0*R_S(\tau) \quad (7)$$

where

$$R_S(\tau)=\left[\int_{-\infty}^{\infty}S^2(t)dt\right]^{-1}\int_{-\infty}^{\infty}S(t)S(t+\tau)dt \quad (8)$$

$$S_0=\int_{-\infty}^{\infty}S_{\rm pump}(t)dt. \quad (9)$$

The amplitude coefficients and time constants a_i and τ_i in (4) and (5) can now be adjusted to fit $\Delta G_{\rm dB}$ and $\Delta\phi$ in (6) and (7) to the pump-probe data. The α-factor can then be calculated from $\Delta G_{\rm dB}$ and $\Delta\phi$ using (1) and (6)

$$\alpha=\frac{-2}{L}\frac{\Delta\phi}{\Delta g}=-20\log(e)\frac{\Delta\phi}{\Delta G_{\rm dB}} \quad (10)$$

and thus the components of the α-factor for each nonlinear physical process can be calculated from the coefficients to the terms in (6) and (7), by using (3),

$$\alpha_{cr}=-20\log(e)\frac{a_{crp}[\rm rad]}{a_{cr}[\rm dB]}$$

$$\alpha_{\rm CH}=-20\log(e)\frac{a_{{\rm CH}p}[\rm rad]}{a_{\rm CH}[\rm dB]}$$

$$\alpha_{\rm inst}=-20\log(e)\frac{a_{{\rm inst}p}[\rm rad]}{a_{\rm inst}[\rm dB]}. \quad (11)$$

Here, the values $a_i[\rm dB]\approx 10\log(a_i+1)$ are the dB values of the linear-scale amplitude and phase coefficients quoted in [6]. Since there is no SHB term in the phase response, henceforth $\alpha_{\rm SHB}=0$.

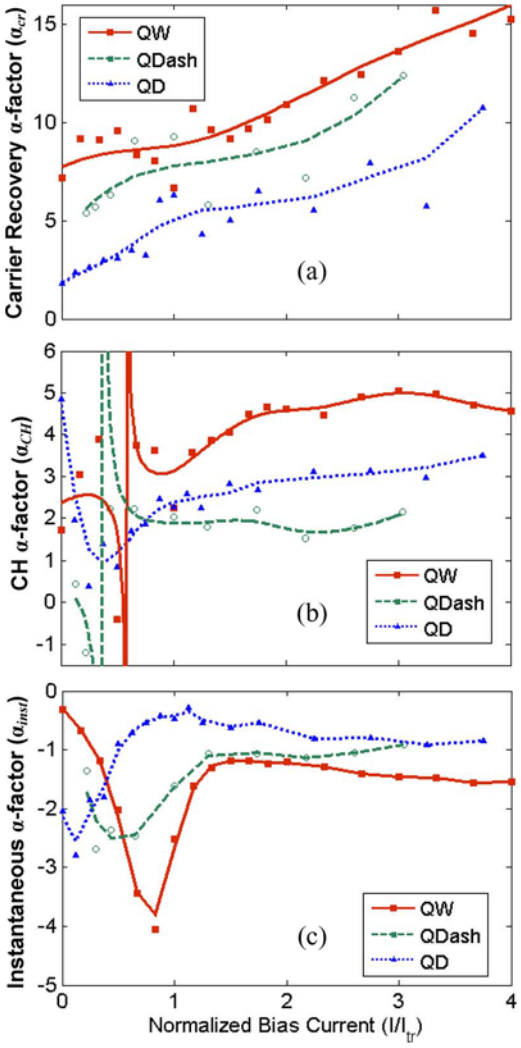

Fig. 2. Comparison of (a) α_{cr}, (b) α_{CH}, and (c) α_{inst} between the QW (squares), and the QDash SOAs (open circles) at 1560 nm, and the QD SOA at 1620 (ES1) (triangles), plotted versus normalized bias current in each amplifier. The lines are the α-factors calculated at all bias currents using smoothing spline fits to the measured amplitude and phase coefficient points.

A. *Analysis of* α_{cr}, α_{CH}, *and* α_{TPA}

We now provide detailed and separate analysis of each α-factor component obtained from our three SOAs, to investigate the effects of increasingly higher dimensionality in the active region. Fig. 2 shows α_{cr}, α_{CH}, and α_{inst} calculated from the data points measured in the three samples using (11), plotted versus bias current normalized to the transparency current (I/I_{tr}). Also shown in the figure are the α-factor curves interpolated to all bias currents, calculated from smoothing spline fits to the measured amplitude and phase coefficient data points. The pump-probe measurements were performed at 1620 nm (ES1) in the QD SOA, and at 1560 nm in the QDash and QW SOA, near the gain peak in each device. The transparency currents I_{tr} for the QD, QDash, and QW samples at these wavelengths were 40 mA, 23 mA, and 15 mA, respectively.

We find the QD SOA has a lower α-factor compared to the QW in all cases, as well as compared to the QDash in all cases except for α_{CH}, making it the most promising for high-speed all-optical signal processing applications. The α_{cr} values in the QD SOA are in the range 2–10, compared to 5–12 in the QDash, and 8–16 in the QW. These QD α_{cr} values at ES1 are about a factor of 2 larger than those reported at the GS in the 1.1-μm InGaAs/GaAs QD SOA in [12]. α_{cr} also shows a consistent increasing trend with bias current in all three SOAs, similar to the findings in [4], [12], [13]. This is attributed to the fact that at high bias current, the gain changes saturate, but the phase changes do not [6].

The values of α_{CH} are fairly constant above transparency, $\sim$3 in the QD SOA, $\sim$4.5 in the QW, and $\sim$2 in the QDash, also slightly larger than values previously measured in bulk SOAs (2 in the AlGaAs bulk SOA in [15], and 0.7 in [4]). The large variations in α_{CH} below transparency we attribute to a changing of the CH process from free-carrier absorption (FCA) heating to stimulated transitions (ST) heating. In the QDash and QW SOAs, ST heating causes the CH coefficients a_{CH} and $a_{\mathrm{CH}p}$ to cross zero and change sign (a switch from carrier heating to carrier cooling) at low bias currents (see [6]). Furthermore, the zero-crossings of a_{CH} and $a_{\mathrm{CH}p}$ do not occur at exactly the same bias current—in both the QDash and QW SOA a_{CH} crosses zero at a higher current than $a_{\mathrm{CH}p}$. This causes the CH α-factor α_{CH} to have an asymptote and take on negative values between the a_{CH} and $a_{\mathrm{CH}p}$ zero-crossings, as observed in Fig. 2(b). This finding has an important implication for reducing chirp effects in lasers, and for reducing phase transients in ultrafast all-optical applications: if a material can be engineered to exhibit carrier cooling for certain bias currents and operating wavelengths, the material can then be made to have zero CH phase transients, or even negative CH phase transients which act to reduce the net transients induced by the other physical processes. Note that we also believe the effects of ST heating are similarly responsible for the variations in α_{CH} in the QD SOA below transparency, but because a_{CH} and $a_{\mathrm{CH}p}$ do not change sign, the variations are less pronounced.

The values of α_{inst}, determined from the coefficients of the instantaneous terms in the impulse response fits, are caused by a combination of two generally indistinguishable effects, TPA and coherent effects [21]. We observe an α_{inst} which is close to -1 in all samples above transparency (~ -0.5 for the QD SOA, ~ -1 for the QDash, and ~ -1.5 for the QW), but which varies significantly below transparency. We know that α_{TPA} due to two-photon-absorption effects alone should be a constant however, since it is by definition proportional to the ratio of the TPA coefficient β_2 and the Kerr coefficient n_2 [22]

$$\alpha_{\mathrm{TPA}} = \frac{4\pi}{\lambda}\frac{n_2}{\beta_2}. \tag{12}$$

Thus, we attribute the variations in our measured values of α_{inst} in Fig. 2 to the presence of coherent artifacts.

Since the coherent artifacts are a result of the probe signal being influenced by the carrier density grating induced in the medium from the coherent interference of the pump-probe pulses [21], [23] (neglecting higher order effects, since the slope of the gain spectrum is low over the bandwidth of the pump light for our experiments performed near the gain peaks),

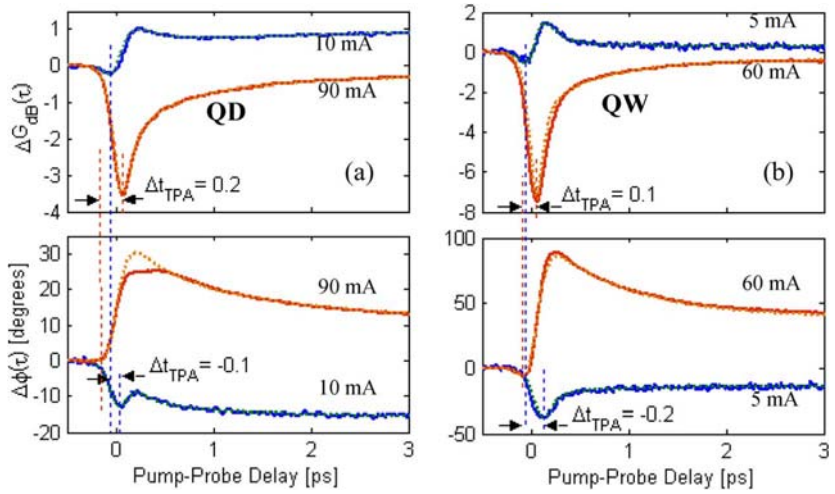

Fig. 3. Amplitude (top row) and phase (bottom row) responses in the (a) QD and (b) QW SOAs obtained from the heterodyne pump-probe measurements for bias currents in both the absorption regime (10 mA in the QD, 5 mA in the QW), and gain regime (90 mA in the QD, and 60 mA in the QW). The dotted lines show the fits to the measured responses. The values of the delay between the minima of the instantaneous dynamics in the amplitude and phase responses, $\Delta t_{\rm TPA}$, are indicated using vertical dashed lines for both bias currents in each sample.

they should be negligible at transparency however. Therefore, we can find the value of $\alpha_{\rm TPA}$ defined in (12) with coherent effects removed by taking the value of $\alpha_{\rm inst}$ at transparency (i.e., $I/I_{\rm tr} = 1$)

$$\alpha_{\rm TPA} = \alpha_{\rm inst}(I_{\rm tr}). \tag{13}$$

We thus find $\alpha_{\rm TPA} \approx -2.5$ for the QW SOA, -1.5 for the Qdash SOA, and -0.5 for the QD SOA.

An additional matter regarding the instantaneous dynamic which is of concern for ultrafast signal processing, and has been previously discussed in the literature, is the temporal offset between the peaks of the amplitude and phase responses near zero delay [4]. Previous studies of the temporal offset were limited to a resolution of >1 ps, and were unable to resolve the delay between the instantaneous TPA dynamics. Here, we find that the peak of the instantaneous dynamic in the amplitude and phase traces occur offset in time with respect to each other by a value $\Delta t_{\rm TPA} = \tau_{\rm min,amp} - \tau_{\rm min,ph} \approx \pm 0.2$ ps. Fig. 3 shows examples of the amplitude and phase ultrafast transients measured in the QD and QW SOAs around zero pump-probe delay, together with their fits. TPA peak offsets of $\Delta t_{\rm TPA} \approx -0.1$ to -0.2 ps are observed in the absorption regime, and $+0.1$ to $+0.2$ ps in the gain regime. These offsets occur because the sharp step changes in the gain and phase occur simultaneously with the instantaneous dynamic and cause its peak to shift to 50–100 fs before (for a positive step) or after (for a negative step) the zero delay point. An offset between the amplitude and phase peaks thus occurs in the absorption and gain regimes because these steps are opposite in sign, but at transparency the delay should be zero.

The TPA dynamic offsets have an impact on the instantaneous α-factor; because of the temporal offset, the α-factor that is actually manifested around zero pump-probe delay can deviate from the values of $\alpha_{\rm inst}$ plotted in Fig. 2(c). This is important to consider when modeling the phase dynamical effects in XPM-based all-optical signal processing devices for example, since the magnitude of the instantaneous phase response may be less than that predicted by the values of $\alpha_{\rm inst}$ calculated without considering the offset, and since the offset would translate to a timing jitter [4]. The effect is also important for optical communication applications, because the temporal nature of the pulse chirp induced by the phase transients impacts the associated dispersion penalty of the link. The dispersion penalty is heavily influenced by the magnitude of the chirp and the position in time within the pulse where it takes place.

Table I summarizes the values measured for α_{cr}, $\alpha_{\rm CH}$, and $\alpha_{\rm TPA}$ together with values previously reported in the literature, as well as the values measured for $\Delta t_{\rm TPA}$ and the recovery times for the associated physical processes, τ_{cr}, $\tau_{\rm CH}$, and $\tau_{\rm SHB}$.

B. Time-Evolution of the Net α-Factor, $\alpha(\tau)$

To further understand the effect of the instantaneous dynamic offset, and to analyze the actual net gain-phase coupling observed in an ultrafast switching device in the first few picoseconds of pump-signal delay, we also plot the time-dependence of the net α-factor $\alpha(\tau)$, calculated from the net changes in gain and index as a function of pump-probe delay τ

$$\alpha(\tau) = -20\log(e)\frac{\Delta\phi(\tau)}{\Delta G_{\rm dB}(\tau)}. \tag{14}$$

$\alpha(\tau)$ is calculated directly from the pump-probe trace data, in the same manner is in [4], [12], and is plotted in Fig. 4 for both the QD and QW SOAs. The plot shows $\alpha(\tau)$ in the time window covering the short-lived CH, SHB, and TPA transients (0–3 ps), and also the window covering the long-lived carrier recovery (3–500 ps).

In the absorption regime, because the instantaneous amplitude response has its minimum before the phase response (a negative $\Delta t_{\rm TPA}$), $\alpha(\tau)$ has a zero crossing followed by an asymptote in both samples, and thus there is a time window where $\alpha(\tau)$ changes sign and has a very large magnitude. In the absorption regime the magnitude of $\alpha(\tau)$ is also larger than $\alpha_{\rm inst}$ around

TABLE I
SUMMARY OF MEASURED α-FACTOR QUANTITIES

Quantity	Unit	QD[a]	QDash[a]	QW[a]	Literature Values
α_{laser}	--	5 – 10	--	2.5 – 5	QD,QW: 0 – 60 [5] and references therein
α_{cr}	--	2 – 10	5 – 12	8 – 16	Bulk: 3 – 12 [4], 7 – 11 [29], 3 – 9 [30], 5 [15] QD: 0.5 – 8 [12], -0.5 – 1 [14], 0 – 3 [24]
τ_{cr}	ps	560 – 80	760 – 290	1500 – 500	--
$\Delta g_{cr,eff}$	ps/cm	800 – -25	1000 – -100	1300 – -400	--
α_{CH}	--	3	2	4.5	Bulk: 0.7 [4], 1.5 [29], 2 [15]
τ_{CH}	ps	1	2 – 1.25	1 – 0.75	--
$\Delta g_{CH,eff}$	ps/cm	-1.2 – -2	10 – -6	0.5 – -3.2	--
α_{TPA}	--	-0.5	-1.5	-2.5	Bulk: -3 [4]
$\Delta g_{inst,eff}$	ps/cm	-2 – -4	-15 – -6	-15 – -9	--
τ_{SHB}	ps	0.25	0.25	0.25 – 0.1	--
$\Delta g_{SHB,eff}$	ps/cm	1.3 – -1.2	4 – -1.5	1.8 – -0.3	--
Δt_{TPA}	ps	-0.1 – 0.2	-0.1 – 0.2	-0.2 – 0.1	--

Ranges of values given are the values from low bias currents (absorption) to high bias currents (gain). The literature values are categorized into measurements made on bulk, QW, or QD SOAs; ps means picosecond.

[a] values reported in this work, measured with ~1 pJ pump pulse energy.

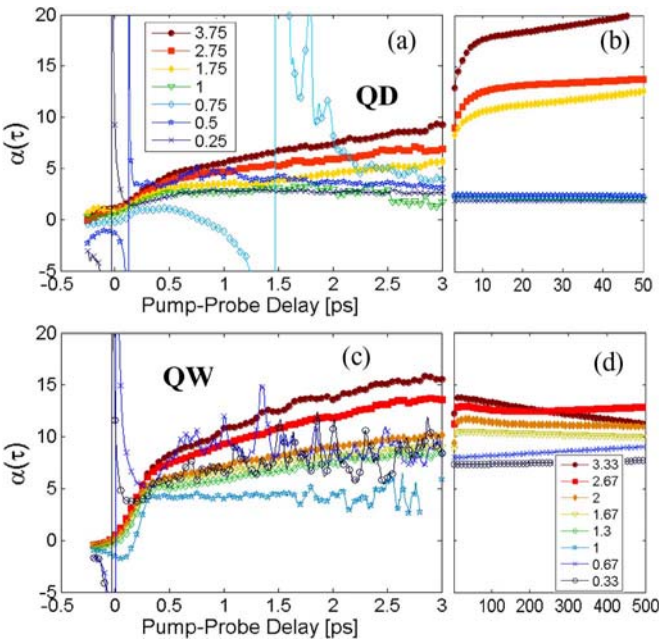

Fig. 4. Instantaneous net α-factor, $\alpha(\tau)$, versus pump probe delay τ, calculated from the pump-probe data in the QD SOA (a), (b), and the QW SOA (c), (d), for different normalized bias currents $I/I_{\rm tr}$. (a), (c) show the $\alpha(\tau)$ curves in the time window when the instantaneous and CH transients are occurring, and (b), (d) show the curves in the time window when only the carrier population is recovering. Separate measurements were needed to measure the two different time windows and the discontinuities at 3 ps are due to imperfect matching of the conditions.

$\tau = 0$ because the magnitude of $\Delta g_{\rm inst}$ is reduced by the addition of the large positive carrier-density step occurring at $\tau = 0$. In the gain regime the opposite effect occurs, since now the instantaneous phase response has its minimum before the gain (a positive $\Delta t_{\rm TPA}$). Thus, $\alpha(\tau)$ changes sign and crosses zero with no asymptote, and is reduced in magnitude because of the large phase step.

Following the effects of the instantaneous transients in the time window $-0.25 < \tau < 0.25$ ps (these values depending on the width and shape of the pump pulses), $\alpha(\tau)$ increases towards the value of α_{cr}, and then settles upon this value once the CH dynamic recovers. Further following this, during the time of the long-lived recovery of the carrier population, $\alpha(\tau)$ should be constant with a value equal to α_{cr}, *unless the amplitude and phase recovery times τ_{cr} and τ_{crp} are not equal*. In the QD SOA, in the gain regime ($\tau_{cr} \equiv \tau_{gr}$, $\tau_{crp} \equiv \tau_{grp}$) $\alpha(\tau)$ in fact increases to values >20 as the carrier population replenishes [Fig. 4(b)], because τ_{grp} is slightly larger than τ_{gr} ($\tau_{grp} \approx 100$ ps, $\tau_{gr} \approx 80$ ps [6]). In the absorption regime ($\tau_{cr} \equiv \tau_{ar}$, $\tau_{crp} \equiv \tau_{arp}$) however, the differences in the recovery times are not large enough to cause a significant change in $\alpha(\tau)$ ($\tau_{arp} \approx \tau_{ar} \approx 575$ ps) thus $\alpha(\tau)$ remains constant. In the QW, interestingly, the behavior is different: in the gain regime τ_{gr} is larger ($\tau_{grp} \approx 450$ ps, $\tau_{gr} \approx 500$ ps) causing $\alpha(\tau)$ to increase, and in the absorption regime τ_{grp} is larger ($\tau_{arp} \approx 2100$ ps, $\tau_{ar} \approx 1500$ ps) causing $\alpha(\tau)$ to decrease. An increase in α-factor during the carrier population recovery was observed in [13], however the reason for the differences in the recovery times is not well understood.

The results of Fig. 4 also confirm that because α_{cr}, $\alpha_{\rm CH}$, and $\alpha_{\rm inst}$ are lower in the QD SOA compared to the QW, the net α-factor $\alpha(\tau)$ at any pump-probe delay within the $\tau < 3$ ps time window is significantly lower in the QD. This indicates significant advantages for high-speed optical communications networks and signal processing applications. When used to amplify signals in optical networks, our QD amplifier would induce less chirp and result in a smaller dispersion penalty. XGM-based signal processing schemes using our QD amplifier would also operate with reduced chirp effects, and the distortions to the

switching window due to the CH, SHB, and instantaneous transients, which come into play at bit rates approaching 1 THz, would be less severe.

C. Effective α-Factor

We can now conclude that the time-resolved net α-factor $\alpha(\tau)$ is dominated largely by the effects of the carrier density changes, i.e., by α_{cr}, since it was found in Section IV-B that $\alpha(\tau)$ is near zero in the time period $\tau < 0.25$ ps, and is still smaller than α_{cr} for $\tau < 3$ ps. This has implications for the behavior of the effective α-factor. Defining the effective, or steady state α-factor as the ratio of the total time-integrated phase change to the total time-integrated gain change

$$\alpha_{\text{eff}}(\tau) = -20\log(e)\frac{\int_{-\infty}^{\infty}\Delta\phi(\tau)d\tau}{\int_{-\infty}^{\infty}\Delta G_{\text{dB}}(\tau)d\tau} = -20\log(e)\frac{\Delta\phi_{\text{eff}}}{\Delta G_{\text{dB,eff}}} \tag{15}$$

we can define effective α-factors for each of the individual nonlinear physical processes as done in (11). In fact, since the recovery times of each nonlinear process are approximately the same in the amplitude and phase responses, the effective α-factors are approximately the same as those in (3) and (11), i.e., $\alpha_{cr,\text{eff}} \approx \alpha_{cr}$, $\alpha_{\text{CH,eff}} \approx \alpha_{\text{CH}}$, and $\alpha_{\text{TPA,eff}} \approx \alpha_{\text{TPA}}$. The approximation is reasonably valid since after performing the integrations in (15) we find that $\alpha_{cr,\text{eff}}$ is at most 30% different from α_{cr}.

These effective α-factors then give the *steady state* total index change and chirp, by taking the sum of the products of each effective α-factor and its corresponding steady-state (time-integrated) gain change $\Delta g_{i,\text{eff}}$, similar to as in (2)

$$\begin{aligned}\Delta\nu_{\text{eff}} &= -\frac{v_g}{\lambda}\Delta n_{\text{eff}} \\ &\approx \frac{v_g}{4\pi}[\alpha_{cr}\Delta g_{cr,\text{eff}} + \alpha_{\text{CH}}\Delta g_{\text{CH,eff}} \\ &\quad + \alpha_{\text{SHB}}\Delta g_{\text{SHB,eff}} + \alpha_{\text{TPA}}\Delta g_{\text{TPA,eff}}]\end{aligned} \tag{16}$$

where

$$\Delta g_{i,\text{eff}} = \frac{\int_{-\infty}^{\infty}\Delta G_{\text{dB}}(\tau)d\tau}{10\log(e)L}. \tag{17}$$

It is readily apparent, however, that the $\alpha_{cr,\text{eff}}\Delta g_{cr,\text{eff}}$ term will be dominant, since the time integral of the carrier recovery gain change will be much larger due to its much longer lifetime. Table I also shows the values of the time integrated gain changes for each of the nonlinear processes in our devices, calculated from the fits to the pump-probe data. Looking at the values we see that the gain change due to carrier heating is at least 100 times less than that due to carrier density changes in the QW SOA, and at least 12 times less in the QD. Also α_{cr} is on average $\sim$2 times larger than α_{CH} (see Fig. 2), therefore $\alpha_{\text{CH,eff}}\Delta g_{\text{CH,eff}}$ will be at least 20 times less than $\alpha_{cr,\text{eff}}\Delta g_{cr,\text{eff}}$. Furthermore the time integral of the instantaneous TPA gain change is simply equal to the value of α_{TPA}, thus it is also comparable to the CH change in magnitude. Thus, we find that the carrier recovery gain change is the dominant nonlinear effect producing steady-state index changes and chirp in our SOAs, i.e., that $\alpha_{\text{eff}} \approx \alpha_{cr}$, and therefore

$$\Delta\nu_{\text{eff}} = -\frac{v_g}{\lambda}\Delta n_{\text{eff}} \approx \frac{v_g}{4\pi}[\alpha_{cr}\Delta g_{cr,\text{eff}}]. \tag{18}$$

This result also suggests that the α_{cr} values should be comparable to the α-factor values obtained from electrical-modulation measurements on lasers below threshold, since the bias modulation frequencies in the majority of these measurement techniques (for example the Hakki–Paoli or AM/FM techniques) are typically less than $1/\tau_{cr}$. We address this issue further in Section V, where we compare the α_{cr} values measured above with measurements in lasers performed with the Hakki–Paoli method.

D. Spectral Dependence of α_{cr}, α_{CH}, and α_{TPA}

The α-factor in QD amplifiers is also believed to potentially vary significantly over the bandwidth of the gain spectrum [8]–[10], [12], [14], due to the excited states creating an asymmetry in the gain spectrum. To study the wavelength dependence of the α-factor in our QD amplifier, we have measured the amplitude and phase dynamics and calculated α_{cr}, α_{CH}, and α_{TPA} as done in Section IV-A at five additional wavelength points within the device gain spectrum. The results are plotted in Fig. 5. The measurements were performed over the same bias current range, 0–150 mA, at each wavelength point, however the transparency current $I_{\text{tr},\lambda i}$ increased as the wavelength was decreased. Although the α-factors varied significantly at each wavelength for the same current, we find that once each curve is plotted versus $I/I_{\text{tr},\lambda i}$, the differences amongst the curves become small (within $\pm$40%), over a wavelength range covering the ground state and the first two excited states. This result suggests that α_{cr}, α_{CH}, and α_{TPA} plotted *as a function of modal gain* are relatively unchanging over the gain spectrum, and indicates a large performance bandwidth for our 1.55-μm QD SOA.

Reports of α-factors in 1.1- and 1.3-μm QD SOAs, although lacking studies of α versus normalized bias or modal gain, appear to still show a larger dependence of α_{cr} on wavelength [12]. We believe that the α-factors in our QD SOA structure are less wavelength dependant because of the "blurring" together of the GS and ES energy levels, due to our QD material's smaller energy level spacings ($\sim$21 meV) and a total homogeneous and inhomogeneous broadening ($\sim$24 meV) that is greater than the level spacing [6]. On the other hand we believe that the close proximity of the excited states and large broadening is also the reason for the relatively larger α-factor values compared to lower wavelength GaAs-based QDs [10], [12].

V. Laser α-Factor

The α-factors in an SOA determined via pump-probe measurements reveal the material gain-index response under optical excitation, and are important for predicting chirp effects in short-pulse amplification, and phase responses in a switching

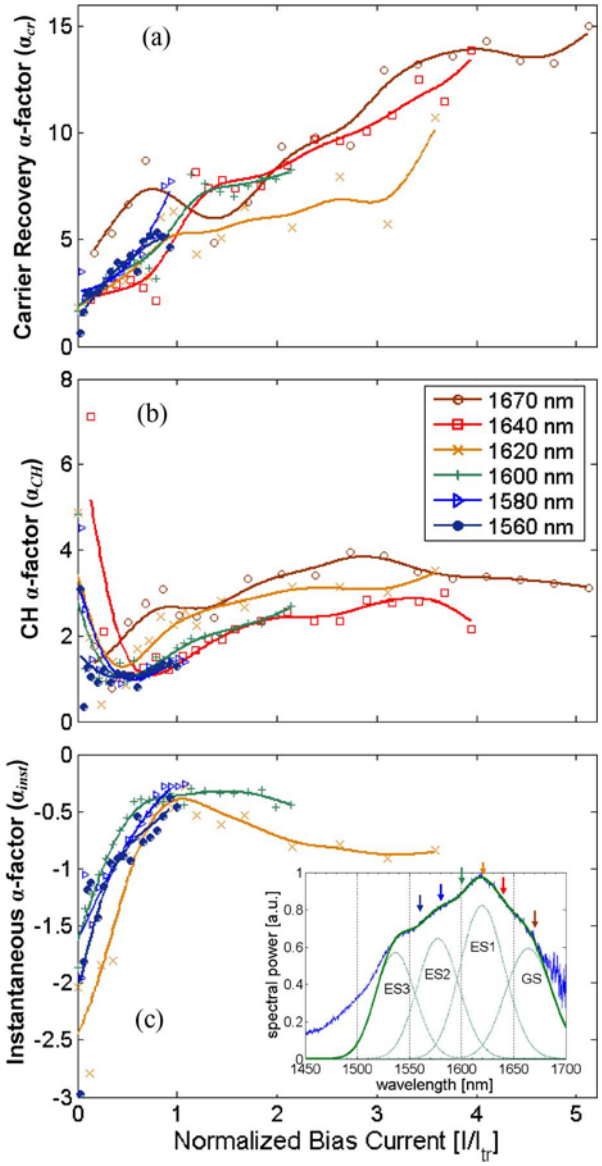

Fig. 5. (a) α_{cr}, (b) $\alpha_{\rm CH}$, and (c) $\alpha_{\rm TPA}$ measured from pump-probe measurements in the QD SOA at six different wavelengths over its gain spectrum. The bias currents are normalized to the transparency currents found at each wavelength (150 mA at 1560 nm, 140 mA at 1580 nm, 70 mA at 1600 nm, 38 mA at 1640 nm, and 30 mA at 1670 nm). The lines are smoothing spline fits to the measured points. The 1620 nm data is identical to that in Fig. 2. In (c) the curves at 1640 nm and 1670 nm are not plotted because at these wavelengths the instantaneous dynamic temporal profile does not match well to a $\rm sech^2$ function due to non-ideal laser pulse shapes produced by the laser at these wavelengths. Inset in (c): QD SOA ASE spectrum at 180 mA, showing contributions from each of the GS and three ESs (dotted green lines), and the fit to the spectrum formed by their sum (solid green line). The arrows show the six measurement wavelengths.

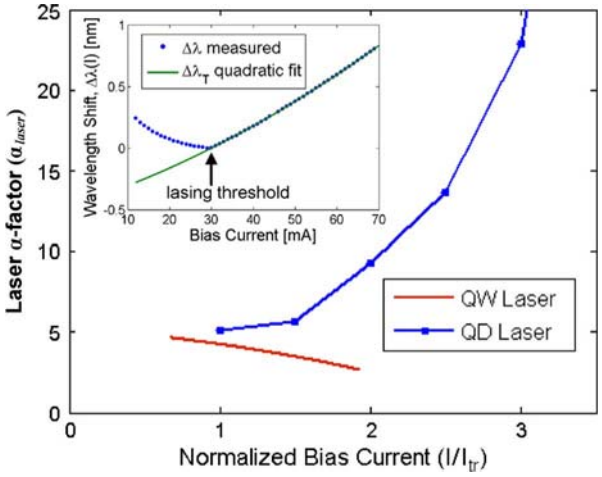

Fig. 6. $\alpha_{\rm laser}$ measured in the matching QD and QW laser samples using the Hakki–Paoli method, versus normalized bias current. Measurements were at the same wavelengths as for α_{cr} in Section IV-A (1560 nm in the QW, 1620 nm in the QD). In the QD the $\alpha_{\rm laser}$ values were only measured at six points and the solid line is a guide to the eye. Inset: Fabry–Perot mode wavelength shift $\Delta\lambda(I)$ measured in the QW laser (blue dots), and quadratic fit to the values above threshold (green solid line) which are the shifts due to thermal effects only, i.e., $\Delta\lambda_T(I)$.

device. It is also important however to characterize the α-factor in lasers, since the α-factor is also an important indicator of chirp effects and linewidth broadening for directly modulated lasers in optical communications systems. How similar the α-factors are between lasers and SOAs of the same structure remains in question however, because of the differences in the modulation mechanism (optical versus electrical) [13], [24], and the differences between "material" and "device" α-factors [25]. For example, the relaxation oscillations created by the presence of laser action are known to greatly influence the nature and magnitude of the chirp [2], [3].

To address this question, we have also performed measurements of the α-factor in QD and QW laser samples, which have the same structure as the SOAs (a ridge width of 2 μm, and a cavity length of 1 mm), but have facets as-cleaved, without AR coatings. The α-factors in these laser samples were measured using the commonly used Hakki–Paoli method, i.e., from measurements of the laser emission spectra for different applied constant-wave (CW) electrical biases below the lasing threshold [26]. Fig. 6 plots the values of $\alpha_{\rm laser}$ calculated from the measurements. The lowest bias currents used in the measurements were $I/I_{\rm tr} = 0.67$ (10 mA) in the QW, and $I/I_{\rm tr} = 1$ (40 mA) in the QD, because below these currents, the Fabry–Perot fringes become indistinguishable from the noise. Lasing occurred at $I/I_{\rm tr} = 2$ (30 mA) in the QW, and the maximum bias applied to the QD laser was $I/I_{\rm tr} = 5$ (200 mA). No lasing was observed in the QD for constant-wave currents up to $I/I_{\rm tr} = 5$ (lasing occurred only with pulsed current at 180 mA).

$\alpha_{\rm laser}$ is obtained by measuring the net modal gain coefficient g, and the wavelength-shift of the peak of the Fabry–Perot modes $\Delta\lambda$, from the laser emission spectra, as a function of the bias current, and by using the equation [26]

$$\alpha_{\rm laser} = -\frac{4\pi}{\lambda}\frac{\dfrac{dn}{dN}}{\dfrac{dg}{dN}} = -\frac{2\pi}{\delta\lambda L}\frac{\dfrac{d\Delta\lambda_N(I)}{dI}}{\dfrac{dg(I)}{dI}} \tag{19}$$

where $\delta\lambda$ is the wavelength spacing between neighboring Fabry–Perot modes, and $\Delta\lambda_N(I)$ is the wavelength-shift of the modes *due to carrier density changes only* (i.e., with the shift due to changes in temperature, $\Delta\lambda_T$, removed). The mode shifts due to changes in temperature were accounted

for by measuring the shift of the fringes due to only thermal effects above threshold, $\Delta\lambda_T(I)$, and subtracting the values of $\mathrm{d}\Delta\lambda_T/\mathrm{d}I$ from the slopes of the total shifts $\mathrm{d}\Delta\lambda(I)/\mathrm{d}I$ below threshold, as described in [26]. The values of $\Delta\lambda(I)$ that were measured are plotted in the inset of Fig. 6. The values of $\Delta\lambda(I)$ were taken to be zero at the lasing threshold (indicated by the arrow in the figure), and the values of $\Delta\lambda_T(I)$ are the values of $\Delta\lambda(I)$ in the QW sample in the 30–70 mA bias-current range, and fit well to a quadratic (green solid line in Fig. 6 inset). The quadratic fit to $\Delta\lambda_T(I)$ was then extrapolated down to 10 mA and up to 200 mA to calibrate out the thermal effects in the QW and QD samples below threshold. The values of $\Delta\lambda_T(I)$ were assumed to be the same in the QD and QW samples, as their structures are matching. The diode resistances $R(I)$ were confirmed to be equal through I-V measurements.

In the QD laser, $\alpha_{\mathrm{laser}} = 5 - 10$ in the bias range $I/I_{\mathrm{tr}} = 1 - 2$. We note that above bias currents of $I/I_{\mathrm{tr}} = 2$ the error in α_{laser} increases as a result of the extrapolation of $\Delta\lambda_T(I)$ to high currents, however a general increasing trend at high bias can still be inferred from the measurements. These α_{laser} values are higher than what has been typically found in GaAs-based QDs using the same technique. This again suggests that the close-spacing of the ES levels in our 1.55-μm QD laser results in a higher α-factor compared to lower-wavelength QD lasers.

The behavior of α_{laser} in the QD structure relative to the QW is also quite different from what was found in the SOAs. The values for the QW laser seen in Fig. 6 in the range $I/I_{\mathrm{tr}} = 0.67 - 2$ are $\alpha_{\mathrm{laser}} = 2.5 - 5$, which are significantly lower than the α_{cr} values found for the QW SOA in Section IV-A in the same current range. α_{laser} in the QW laser is also lower than in the QD laser, particularly at high bias, in contrast to the finding in Section IV-A that α_{cr} is higher in the QW SOA. Furthermore in the QW the values of α_{laser} have a decreasing trend instead of an increasing trend. These α_{laser} values in fact are in the range more typically found in QW lasers using the same technique [9], [26]–[28].

The large differences between α_{laser} and α_{cr} confirm there is a disparity between α-factors measured in lasers and SOAs. We believe the dissimilarities result from the differences in the carrier modulation mechanism (electrical bias modulation versus optical gain modulation) [13] and [24], and differences in the measurement technique. α-factors that are lower under electrical modulation than under optical modulation agree with the findings in [13] and [24]. We believe the differences in the carrier modulation mechanism can cause differences in the α-factor for a number of reasons:

- In the SOAs, optical pulses modulate the resonant carrier population directly, whereas changes in the electrical bias in the lasers modulate the carrier population at states near the electrodes which are spatially and energetically displaced from the optically resonant state, as mentioned in [12].
- In pump-probe measurements the optical pulses modulate the carrier population only in the small area where the optical mode overlaps the dot or well layers, whereas in the lasers, changes in the electrical bias change the carrier population over the mode's entire cross-sectional area.
- The pump pulses change the carrier population non-uniformly along the length of the waveguide, since the pump intensity exponentially decays or grows as it propagates, whereas in the bias modulation case the carrier population is changed homogeneously along the length of the waveguide.
- The carrier density changes caused by the pump pulses occur in a spectral region covering their broad 30 nm bandwidth, whereas α_{laser} is calculated using data averaged over only a $\sim$2 nm range.

This disparity between the SOA and laser α-factors has important implications for directly modulated laser applications. Our QD structure shows a lower α-factor as an all-optical device, but a higher α-factor as an electrically modulated laser, indicating that our QW structure may instead provide for lower chirp and better high-speed performance as a directly modulated laser. Further study of the differences between the gain-index coupling under electrical and optical modulation conditions are needed to better understand the cause for the differences between the SOA and laser α-factors, and to clarify how much of a role the dissimilarities between the measurement techniques, and the difficulties associated with the CW Hakki–Paoli measurements, play in causing these differences.

VI. Conclusion

We have reported measurements of the time-resolved linewidth enhancement factors α_{cr}, α_{CH}, and α_{TPA} in a zero-dimensional InAs/InGaAsP/InP QD structure operating near 1.55-μm-wavelengths, and have compared them to one-dimensional QDash and matching two-dimensional QW structures also operating at this wavelength. These α-factors broken down into values for each nonlinear effect are important for use in modeling of the phase dynamics and chirp in all-optical signal processing devices, and for assessing the performance of directly modulated lasers in optical communications systems.

We have found α_{cr} values which are the lowest in the QD SOA ($\alpha_{cr} = 2 - 10$), and the highest in the QW ($\alpha_{cr} = 8 - 16$), confirming that the 0-D QD structure provides for the lowest α-factor due to its more symmetrical delta-function-like density of states. α_{cr} also consistently increases with increasing bias, in agreement with past findings.

The α-factors for the ultrafast processes of CH and TPA were also lower in the QD compared to the matching QW. The value of α_{TPA} was different from α_{inst}, and was isolated from the influence of coherent effects by taking the value of α_{inst} at the transparency current. Also, at high biases the net α-factor the device actually exhibits around zero delay is lower than α_{TPA} and α_{inst}, because of the temporal offset of the amplitude and phase responses, and the additive effects of the long-lived step change. Lower ultrafast α_{CH} and α_{TPA} factors at biases above transparency show that our QD device can provide for improved chirp performance and reduced phase transients when biased in the gain regime in ultrahigh-speed all-optical applications incorporating bit-rates approaching 1 THz. Also, in a narrow window of low bias currents our QDash and QW structures exhibited zero and negative α_{CH} values, due to the presence of carrier cooling, indicating the possibility of low-chirp performance and

reduced ultrafast phase transients in these structures under certain conditions.

Examination of the net α-factor $\alpha(\tau)$ also found that the effects of ultrafast carrier heating and TPA on the effective α-factor are relatively small. As such the effective steady state α-factor is dominated by long-lived carrier density changes, i.e., $\alpha_{\text{eff}} \approx \alpha_{cr}$. This implies that for low bit-rate ($<$1 GHz) or CW applications the α-factor is dominated by α_{cr}.

Our 1.55-μm QD amplifier does not have an ultralow α-factor as seen in some other 1.1–1.3-μm or tunnel-injection QD structures however. This may be ascribed to its relatively close energy level spacing (on the order of the total inhomogeneous and homogeneous broadening). On the other hand the α-factor values show little wavelength dependence over the QD gain spectrum. Thus, these InAs/InGaAsP/InP QDs maintain their high-speed performance properties over a wide bandwidth. This broader-bandwidth capability is an important additional enhancement over QW structures.

It is also important to note however that there are large variations in α as a function of bias current, stressing the fact that the phase effects of a laser or SOA device cannot be quantified by quoting a single α-factor value. Often the minimum low-current α-factor only is quoted, but since many applications require operation at high bias where the α-factor may be significantly larger, such a practice would result in underestimation of the chirp penalties in an operational system.

Finally, we found that the α-factor values measured in matching laser structures were significantly different from the pump-probe SOA α-factors. In the lasers the values in the QD ($\alpha_{\text{laser}} = 5-10$) were higher than in the QW ($\alpha_{\text{laser}} = 3-4.5$). Thus, it is evident from this study that the value of the α-factor depends on whether the device is modulated electrically or optically. Because of these differences, our QD structure as an SOA shows a lower α-factor than the QW, but as a laser it shows a higher α-factor. This indicates the QW structure could still provide for lower chirp and better high-speed performance as a directly modulated laser.

These results highlight that lower chirp, reduced phase transients, and broader bandwidth performance in all-optical applications can be achieved by moving to InP-based QDs at 1.55-μm wavelengths. It is also evident however that further improvements in the high-speed performance of these QDs can come from future work on such things as engineering of the energy level structure and introducing tunnel injection, as well as further study of the effects of electrical versus optical gain modulation.

ACKNOWLEDGMENT

A. J. Zilkie would like to acknowledge M. Y. Xu for helpful discussions.

REFERENCES

[1] C. H. Henry, "Theory of the linewidth of semiconductor-lasers," *IEEE J. Quantum Electron.*, vol. 18, no. 2, pp. 259–264, Feb. 1982.

[2] I. Tomkos, D. Chowdhury, J. Conradi, D. Culverhouse, K. Ennser, C. Giroux, B. Hallock, T. Kennedy, A. Kruse, S. Kumar, N. Lascar, I. Roudas, M. Sharma, R. S. Vodhanel, and C. C. Wang, "Demonstration of negative dispersion fibers for DWDM metropolitan area networks," *IEEE J. Sel. Topics Quantum Electron.*, vol. 7, no. 3, pp. 439–460, May–Jun. 2001.

[3] K. Hinton and T. Stephens, "Modeling high-speed optical-transmission systems," *IEEE J. Sel. Areas Commun.*, vol. 11, no. 3, pp. 380–392, Apr. 1993.

[4] J. Wang, A. Maitra, C. G. Poulton, W. Freude, and J. Leuthold, "Temporal dynamics of the alpha factor in semiconductor optical amplifiers," *J. Lightw. Technol.*, vol. 25, no. 3, pp. 891–900, Mar. 2007.

[5] J. M. Vazquez, H. H. Nilsson, J. Z. Zhang, and I. Galbraith, "Linewidth enhancement factor of quantum-dot optical amplifiers," *IEEE J. Quantum Electron.*, vol. 42, no. 10, pp. 986–993, Oct. 2006.

[6] A. J. Zilkie, J. Meier, M. Mojahedi, P. J. Poole, P. Barrios, D. Poitras, T. J. Rotter, C. Yang, A. Stintz, K. J. Malloy, P. W. E. Smith, and J. S. Aitchison, "Carrier dynamics of quantum-dot, quantum-dash, and quantum-well semiconductor optical amplifiers operating at 1.55 μm," *IEEE J. Quantum Electron.*, vol. 43, no. 11, pp. 982–991, Nov. 2007.

[7] Z. Mi, P. Bhattacharya, and J. Yang, "Growth and characteristics of ultralow threshold 1.45 μm metamorphic InAs tunnel injection quantum dot lasers on GaAs," *Appl. Phys. Lett.*, vol. 89, pp. 153109-1–153109-3, Oct. 2006.

[8] S. Fathpour, P. Bhattacharya, S. Pradhan, and S. Ghosh, "Linewidth enhancement factor and near-field pattern in tunnel injection $In_{0.4}Ga_{0.6}As$ self-assembled quantum dot lasers," *Electron. Lett.*, vol. 39, pp. 1443–1445, Oct. 2003.

[9] A. A. Ukhanov, A. Stintz, P. G. Eliseev, and K. J. Malloy, "Comparison of the carrier induced refractive index, gain, and linewidth enhancement factor in quantum dot and quantum well lasers," *Appl. Phys. Lett.*, vol. 84, pp. 1058–1060, Feb. 2004.

[10] D. Rodriguez, I. Esquivias, S. Deubert, J. P. Reithmaier, A. Forchel, M. Krakowski, M. Calligaro, and O. Parillaud, "Gain, index variation, and linewidth-enhancement factor in 980-nm quantum-well and quantum-dot lasers," *IEEE J. Quantum Electron.*, vol. 41, no. 2, pp. 117–126, Feb. 2005.

[11] C. Y. Tsai, C. H. Chen, T. L. Sung, C. Y. Tsai, and J. M. Rorison, "Theoretical modeling of carrier and lattice heating effects for frequency chirping in semiconductor lasers," *Appl. Phys. Lett.*, vol. 74, pp. 917–919, Feb. 1999.

[12] S. Schneider, P. Borri, W. Langbeina, U. Woggon, R. L. Sellin, D. Ouyang, and D. Bimberg, "Linewidth enhancement factor in InGaAs quantum-dot amplifiers," *IEEE J. Quantum Electron.*, vol. 40, no. 10, pp. 1423–1429, Oct. 2004.

[13] M. van der Poel, E. Gehrig, O. Hess, D. Birkedal, and J. M. Hvam, "Ultrafast gain dynamics in quantum-dot amplifiers: Theoretical analysis and experimental investigations," *IEEE J. Quantum Electron.*, vol. 41, no. 9, pp. 1115–1123, Sep. 2005.

[14] J. Kim and S. L. Chuang, "Theoretical and experimental study of optical gain, refractive index change, and linewidth enhancement factor of p-doped quantum-dot lasers," *IEEE J. Quantum Electron.*, vol. 42, no. 9, pp. 942–952, Sep. 2006.

[15] C. T. Hultgren and E. P. Ippen, "Ultrafast refractive-index dynamics in algaas diode-laser amplifiers," *Appl. Phys. Lett.*, vol. 59, pp. 635–637, Aug. 1991.

[16] A. Mecozzi and J. Mork, "Saturation effects in nondegenerate four-wave mixing between short optical pulses in semiconductor laser amplifiers," *IEEE J. Sel. Topics Quantum Electron.*, vol. 3, no. 5, pp. 1190–1207, Oct. 1997.

[17] G. P. Agrawal and N. A. Olsson, "Self-phase modulation and spectral broadening of optical pulses in semiconductor-laser amplifiers," *IEEE J. Quantum Electron.*, vol. 25, no. 11, pp. 2297–2306, Nov. 1989.

[18] J. Mork and J. Mark, "Time-resolved spectroscopy of semiconductor laser devices: Experiments and modeling," *Proc. SPIE*, vol. 2399, pp. 146–159, 1995.

[19] A. J. Zilkie, J. Meier, P. W. E. Smith, M. Mojahedi, J. S. Aitchison, P. J. Poole, C. N. Allen, P. Barrios, and D. Poitras, "Femtosecond gain and index dynamics in an InAs/InGaAsP quantum dot amplifier operating at 1.55 μm," *Opt. Express*, vol. 14, pp. 11453–11459, Nov. 2006.

[20] K. L. Hall, G. Lenz, A. M. Darwish, and E. P. Ippen, "Subpicosecond gain and index nonlinearities in InGaAsP diode-lasers," *Opt. Commun.*, vol. 111, pp. 589–612, Oct. 1994.

[21] P. Borri, F. Romstad, W. Langbein, A. E. Kelly, J. Mork, and J. M. Hvam, "Separation of coherent and incoherent nonlinearities in a heterodyne pump-probe experiment," *Opt. Express*, vol. 7, pp. 107–112, Jul. 2000.

[22] J. Mork and A. Mecozzi, "Theory of the ultrafast optical response of active semiconductor waveguides," *J. Opt. Soc. Am. B.*, vol. 13, pp. 1803–1816, Aug. 1996.

[23] A. Mecozzi and J. Mork, "Theory of heterodyne pump-probe experiments with femtosecond pulses," *J. Opt. Soc. Am. B.*, vol. 13, pp. 2437–2452, Nov. 1996.

[24] M. van der Poel, D. Birkedal, J. Hvam, M. Laemmlin, and D. Bimberg, "Alpha parameter in quantum-dot amplifier under optical and electrical carrier modulation," presented at the Conf. Lasers and Electro-Optics (CLEO), San Francisco, CA, May 16–21, 2004.

[25] A. Martinez, A. Lemaitre, K. Merghem, L. Ferlazzo, C. Dupuis, A. Ramdane, J.-G. Provosta, B. Dagens, O. L. Gouezigou, and O. Gauthier-Lafaye, "Static and dynamic measurements of the alpha-factor of five-quantum-dot-layer single-mode lasers emitting at 1.3 μm on GaAs," *Appl. Phys. Lett.*, vol. 86, pp. 211115-1–211115-3, 2005.
[26] A. Schonfelder, S. Weisser, J. D. Ralston, and J. Rosenzweig, "Alpha-factor improvements in high-speed P-doped $In_{0.35}Ga_{0.65}As$/GaAs MQW lasers," *Electron. Lett.*, vol. 29, pp. 1685–1686, Sep. 1993.
[27] J. Stohs, D. J. Bossert, D. J. Gallant, and S. R. J. Brueck, "Gain, refractive index change, and linewidth enhancement factor in broad-area GaAs and InGaAs quantum-well lasers," *IEEE J. Quantum Electron.*, vol. 37, no. 11, pp. 1449–1459, Nov. 2001.
[28] D. J. Bossert and D. Gallant, "Gain, refractive index, and α-parameter in InGaAs-GaAs SQW broad-area lasers," *IEEE Photon. Technol. Lett.*, vol. 8, no. 3, pp. 322–324, Mar. 1996.
[29] R. Giller, R. J. Manning, and D. Cotter, "Gain and phase recovery of optically excited semiconductor optical amplifiers," *IEEE Photon. Technol. Lett.*, vol. 18, no. 9, pp. 1061–1063, May 2006.
[30] I. Kang and C. Dorrer, "Measurements of gain and phase dynamics of a semiconductor optical amplifier using spectrograms," presented at the Optical Fiber Commun. Conf. (OFC), Los Angeles, CA, 2004, Paper MF43.

Aaron J. Zilkie (S'98–M'07) was born in Winnipeg, Manitoba, Canada, in 1978. He received the B.Sc. degree in electrical engineering from the University of Manitoba, Winnipeg, Manitoba, in 2001, and the M.A.Sc. degree in electrical and computer engineering from the University of Toronto, Toronto, ON, Canada, where he is currently working toward the Ph.D. degree in electrical and computer engineering.

He interned at Nortel Networks, Ottawa, ON, Canada, from 1999 to 2000 in the optical networks division before beginning his M.A.Sc. degree. His current research interests include semiconductor quantum dot (QD) devices, SOAs for all-optical switching, and nonlinear processes in semiconductor materials and their applications.

Mr. Zilkie is a member of the Optical Society of America.

Joachim Meier received the degree of Dipl.-Ing. (FH) in electrical engineering from the University of Applied Science, Regensburg, Germany, in 1998, the M.S. degree in optics in 2000, and the Ph.D. degree in optics in 2004 from the College of Optics at the University of Central Florida, Orlando.

He is currently with High Q Laser Production, Austria.

Mo Mojahedi (M'98–SM'07) received the Ph.D. degree from the Center for High Technology Materials (CHTM) at the University of New Mexico (UNM), Albuquerque, in December 1999. He was the recipient of the Popejoy award for the outstanding doctoral dissertation in physics and engineering at UNM for the years 1997–2000.

Immediately after his Ph.D., he worked as a Research Assistant Professor at CHTM. In August 2001, he joined the Faculty of Electrical and Computer Engineering at the University of Toronto, ON, Canada. His research interests span a wide range of topics which includes, matter wave interactions, abnormal velocities, meta-materials, photonic crystals, dispersion engineering, quantum dots and wells lasers, fundamental electromagnetic theory, macro and nanoscale microwave and photonic devices.

Amr S. Helmy (M'99–SM'06) received the B.Sc. degree from Cairo University, Cairo, Egypt, in 1993, in electronics and telecommunications engineering. He received the M.Sc. and Ph.D. degrees from the University of Glasgow, Scotland, U.K., with a focus on photonic fabrication technologies, in 1999 and 1994, respectively.

He is an Assistant Professor in the Department of Electrical and Computer Engineering at the University of Toronto, Toronto, Ontario, Canada. Prior to his academic career, he held a position at Agilent Technologies photonic devices, R&D division, in the U.K. At Agilent, his responsibilities included developing distributed feedback lasers, monolithically integrated lasers, modulators and amplifiers in InP-based semiconductors. He also developed high-powered submarine-class 980 nm InGaAs pump lasers. His research interests include photonic device physics and characterization techniques, with emphasis on nonlinear optics in III-V semiconductors; applied optical spectroscopy in III-V optoelectronic devices and materials; III-V fabrication and monolithic integration techniques.

Dr. Helmy is a member of the Optical Society of America.

Philip J. Poole received the B.Sc. degree in physics and the Ph.D. degree from Imperial College, University of London, London, U.K., in 1989 and 1993, respectively.

He joined the National Research Council of Canada, Ottawa, Ontario, Canada, in 1993, working on the optical properties of semiconductors concentrating on the application of quantum well intermixing to optical device integration. In 1996, he switched to the growth of InP-based semiconductor structures using chemical beam epitaxy for both optoelectronic devices and fundamental studies. These include the study of the growth of self-assembled quantum dots and selective area epitaxy for the creation of novel nanostructures.

Pedro Barrios received the B.Sc. degree in electronic engineering from the IUPFAN, Venezuela, in 1989, and the M.S. and Ph.D. degrees in electrical engineering from the University of Pittsburgh, Pittsburgh, PA, in 1993 and 1997, respectively.

He worked as a Postdoc at the NanoFAB Center of Texas A&M University during 1998–1999 and at the Electrical Engineering Department of the University of Notre Dame from 1999 to 2000. Currently, he works for the Nanofabrication group at the Institute for Microstructural Sciences of the National Research Council of Canada, Ottawa, ON, Canada. He is currently pursuing research in fabrication of electronic and optoelectronic devices on Si, and III-Vs semiconductors. He has also investigated the oxidation of III-V native oxides (AIGaAs and InAlP) with focus in materials, fabrication and characterization of MOS and HEMT devices, as well as underwent research in electronic materials characterization and development of thin films and nanostructure devices on Si.

Dr. Barrios is a member of the Materials Research Society.

Daniel Poitras received the Ph.D. degree from École Polytechnique de Montréal, Canada, in 2000, where he worked on plasma-deposited inhomogeneous optical coatings.

He is a research officer at the National Research Council of Canada, Ottawa, ON, Canada. His interests cover all the research aspects of optical coatings (new applications, theory, design, fabrication and characterization).

Thomas J. Rotter (M'07) received the M.S. degree in physics from the Westphaelische Wilhelms-Universitaet Muenster, Muenster, Germany, in 1997. He is currently pursuing the Ph.D. degree at the University of New Mexico (UNM), Albuquerque.

In 1998, he joined the Center for High Tech Materials, UNM. His research work includes ultrashort pulse lasers, MBE growth of semiconductor materials, semiconductor lasers and self-assembled quantum nanostructures.

Mr. Rotter is a member of the Optical Society of America.

Chi Yang was born in Henan, China, in 1975. He received the B.E. degree in optical engineering from Zhejiang University, Hangzhou, China, in 1996, and the M.S. degree in optics from Shanghai Institute of Optics and Fine Mechanics, Chinese Academy of Sciences (CAS), Shanghai, China, in 1999. He is currently working toward the Ph.D. degree in electrical engineering at the University of New Mexico, Albuquerque.

His research interests include quantum dot VCSEL, strained quantum well lasers and high-power lasers.

Andreas Stintz was born in Merseburg, Germany, in 1964. He received the Ph.D. degree in physics from the University of New Mexico, Albuquerque, in 1993. The subject of his dissertation was field desorption phenomena.

From 1994 to 1995, he was a Postdoctoral Fellow with the Department of Physics and Astronomy, University of New Mexico, where he investigated the singlet D resonance in the ion. In 1996, he joined the Center for High Technology Materials and became involved in crystal growth for III-V semiconductors by molecular beam epitaxy. His research includes high-power quantum-well lasers, quantum dot lasers and detectors, saturable absorbers, and crystal growth on metamorphic buffer layers. He also cofounded Zia Laser, Inc., in 2000, a start-up company with the goal of marketing a new generation of telecom and datacom lasers.

Kevin J. Malloy received the B.S.E.E. degree from the University of Notre Dame, Notre Dame, IN, in 1978, the M.S.E.E. degree in 1980 and the Ph.D. degree in electrical engineering from Stanford University, Stanford, CA, in 1984.

He served as a Program Manager at the Air Force Office of Scientific Research from 1983–1988. After a term as a Visiting Professor at the University of California, Berkeley, he joined the faculty of the Department of Electrical and Computer Engineering, University of New Mexico (UNM), Albuquerque, as a member of the Center for High Technology Materials. He currently serves as Associate Dean for Research for the School of Engineering at UNM. His research interests include the materials science and physics of semiconductor structures and waves in periodic media.

Peter W. E. Smith (M'67–SM'76–F'78–LF'03) was born in London on November 3, 1937. He received the B.Sc. degree in mathematics and physics in 1958 and the M.Sc. and Ph.D. degrees in physics in 1961 and 1964, respectively, all from McGill University, Montreal, QC, Canada. His thesis work was on the paramagnetic relaxation of iron group ions in dilute single crystals.

From 1958 to 1959, he was an Engineer at the Canadian Marconi Company, Montreal, Canada, where he worked on transistor circuitry. After receiving the Ph.D. degree, he joined Bell Telephone Laboratories, Holmdel, NJ, where he conducted research on laser mode selection and mode-locking, pioneered the development of waveguide gas lasers, and demonstrated and developed hybrid bistable optical devices. In 1970, he spent nine months at the University of California, Berkeley, as Visiting Mackay Lecturer in the Department of Electrical Engineering, and in 1978–1979 he was a Visiting Research Scientist at the Laboratoire d'Optique Quantique, Ecole Polytechnique, Palaiseau, France. From 1984 to 1992, he was with Bell Communications Research, Red Bank, NJ, where for the last three years he was Division Manager of Photonic Science and Technology Research. In July 1992, he became a Professor of electrical and computer engineering at the University of Toronto, Toronto, ON, Canada. From 1992 to 1995 he served as Executive Director of the Ontario Laser and Lightwave Research Centre, and from 1999 to 2003 as Director of the Nortel Institute for Telecommunications at the University of Toronto. Since 2003 he has been Professor Emeritus at the University of Toronto, and has pursued research interests in photonics involving fibre Bragg grating devices, ultrafast optical switching, and nonlinear optical properties of nanocrystals. He has published over 300 technical papers in refereed journals and conference proceedings (with over 6000 citations listed in the ISI Science Citations Index), and holds 34 patents in the photonics area.

Dr. Smith is a Fellow of the Optical Society of America, and the Institute of Physics (UK). He is a member of the American Physical Society, and the Canadian Association of Physicists. He has participated in numerous conference organizing committees and has been guest editor for several special journal issues. He served as associate editor of the IEEE JOURNAL OF QUANTUM ELECTRONICS 1976–1979; associate editor of Optics Letters 1980–1982; and editor of Optics Letters 1991–1995. From 1987 to 1991, he served as editor-in-chief of the IEEE Press book series *Progress in Lasers and Electro-Optics*, and from 1996–1998 as Chair of the Board of Editors of the Optical Society of America. He was the founder of the OSA/IEEE Photonic Switching Conference and served as co-Chair of the first two conferences in 1987 and 1989. He served as president of the IEEE Lasers and Electro-Optics Society in 1984, and was from 1993–1997 a member of the Board of Directors of the Optical Society of America. In 1986, he was awarded the IEEE Quantum Electronics Award, and in 2000, the IEEE Third Millennium Medal.

J. Stewart Aitchison (M'96–SM'00) received the B.Sc. degree (with first class honors) and the Ph.D. degree in physics from Heriot-Watt University, Edinburgh, U.K., in 1984 and 1987, respectively. His dissertation research was on optical bistability in semiconductor waveguides.

From 1988 to 1990 he was a Postdoctoral Member of Technical Staff at Bellcore, Red Bank, NJ. His research interests were in high nonlinearity glasses and spatial optical solitons. He then joined the Department of Electronics and Electrical Engineering, University of Glasgow, U.K., in 1990 and was promoted to a personal chair as Professor of Photonics in 1999. His research was focused on the use of the half band gap nonlinearity of III-V semiconductors for the realization of all-optical switching devices and the study of spatial soliton effects. He also worked on the development of quasi phase matching techniques in III-V semiconductors, monolithic integration, optical rectification, and planar silica technology. His research group developed novel optical biosensors, waveguide lasers and photosensitive direct writing processes based around the use of flame hydrolysis deposited (FHD) silica. In 1996 he was the holder of a Royal Society of Edinburgh Personal Fellowship and carried out research on spatial solitons as a visiting researcher at CREOL, University of Central Florida. Since 2001 he has held the Nortel chair in Emerging Technology, in the Department of Electrical and Computer Engineering at the University of Toronto, Toronto, ON, Canada. His research interests cover all-optical switching and signal processing, optoelectronic integration and optical bio-sensors. His research has resulted in seven patents, around 185 journal publications, and 200 conference publications. From 2004 to 2007 he was the Director of the Emerging Communications Technology Institute at the University of Toronto. Since 2007 he has been Vice Dean of Research for the Faculty of Applied Science and Engineering, University of Toronto.

Dr. Aitchison is a Fellow of the Optical Society of America and a Fellow of the Institute of Physics London.